



## Formulation of an Ideal Solid Oxide Fuel Cell

Sarwan S. Sandhu<sup>1\*</sup>, Kevin R. Hinkle<sup>2</sup>

<sup>1,2</sup>Department of Chemical and Materials Engineering, The University of Dayton, 300 College Park, Dayton, OH 45469-0246, USA

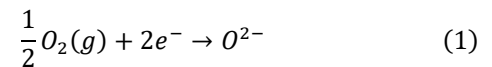
ARTICLE INFO	ABSTRACT
Published Online: 26 March 2024	Principles of transport phenomena and chemical/ electrochemical reaction kinetics were employed to develop the formulation for the prediction of fuel (e.g., $H_2(g)$ ) and oxidant (e.g., $O_2(g)$ ) mole fraction profiles in the porous anode and cathode electrodes of an ideal solid oxide fuel cell (SOFC). The ideal SOFC is composed of the porous anode, <i>A</i> , which is the cermet of metallic nickel and yttria-stabilized zirconia and the porous cathode, <i>C</i> , which is the strontium-doped lanthanum manganite. A thin film of the yttria-stabilized zirconia is the solid electrolyte separating the cell electrodes. The cell anode-side fuel and cathode-side oxidant supply compartments are continuously stirred to maintain constant concentrations of fuel and oxidant in them.
Corresponding Author: <b>Sarwan S. Sandhu</b>	The relevant analytical formulation as well as the numerical data computed is presented. The current calculated data show a non-linear decrease, associated with the coupled effect of diffusion and consumption, in the mole fractions of hydrogen and oxygen in the porous electrodes with an increase in the distance from the reactant supply compartments towards the cell electrolyte separator.

### 1. INTRODUCTION

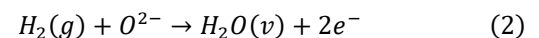
The work reported in this presentation is continuation of that reported for the steady-state [1] and non-steady state [2] utilization of both fuel, hydrogen, and oxidant, oxygen from air. The system modeled here is sketched in Figure 1. It is composed of the SOFC anode, *A*, electrolyte separator, *Electro*, and cathode, *C*. The cell anode is the cermet of metallic nickel,  $NiO(s)$ , and yttria,  $Y_2O_3(s)$ , – stabilized zirconia,  $ZrO_2(s)$ , with 16 – 30% porosity to facilitate the transport of reactant and product species. The electrolyte separator between the cell electrodes, *Electro*, is a thin film of the yttria-stabilized zirconia. The yttria doping is required to stabilize the cubic crystal structure of zirconia as well as for the creation of oxygen-vacancy defects required for the enhancement of ionic transport of the oxide anions,  $O^{2-}(s)$ . A typical composition of the solid oxide electrolyte is: yttria (16.9%) and zirconia (83.1%) by weight [3]. The cell cathode, *C*, is the porous strontium-doped lanthanum manganite,  $La_{1-x}Sr_xMnO_3(s)$ , with  $x \in [0.1, 0.18]$ , a *p*-type semiconductor. The strontium doping bestows the *p*-type electronic conductivity by the creation of electron holes. Other materials; particularly, *p*-type conducting perovskite structures display mixed electronic and ionic conductivity. The

perovskites; lanthanum strontium ferrite, lanthanum strontium cobaltite as well as *n*-type semiconductors are better electrocatalysts than the state-of-the art lanthanum manganite [4]. The range of the cathode porosity is (20-40%) for rapid mass transport of reactant /product species.

In the SOFC cathode, shown in the sketch of **Figure 1**, the oxide anions are generated via the following electrochemical reaction:



The oxide ions migrate through the electrolyte separator for their consumption in the cell porous anode via the following electrochemical reaction:



The SOFC is assumed to be operated at a constant current level to deliver required electric power to an external electrical load under the isothermal and isobaric conditions. The cell anode-side fuel compartment is fed from a fuel (e.g., hydrogen gas) storage tank. The mixture of the gaseous fuel and water vapor product species of reaction (2) is stirred to maintain the same fuel concentration level throughout the fuel-side compartment. The fuel and water vapor mixture is assumed to be continuously sent to a semi-permeable membrane (SPM) to remove water vapor and other chemical species, harmful to the

## “Formulation of an Ideal Solid Oxide Fuel Cell”

electrochemical reaction (2), to maintain a required constant pressure in the fuel compartment. The oxidant (oxygen gas of the air) feed to the cathode-side compartment is under the steady-state, isothermal and isobaric conditions. Also, the

cathode-side oxidant compartment is stirred to maintain the same oxygen concentration level throughout the oxidant compartment. The cell formulation for the SOFC performance analysis /design is provided in Section 2.

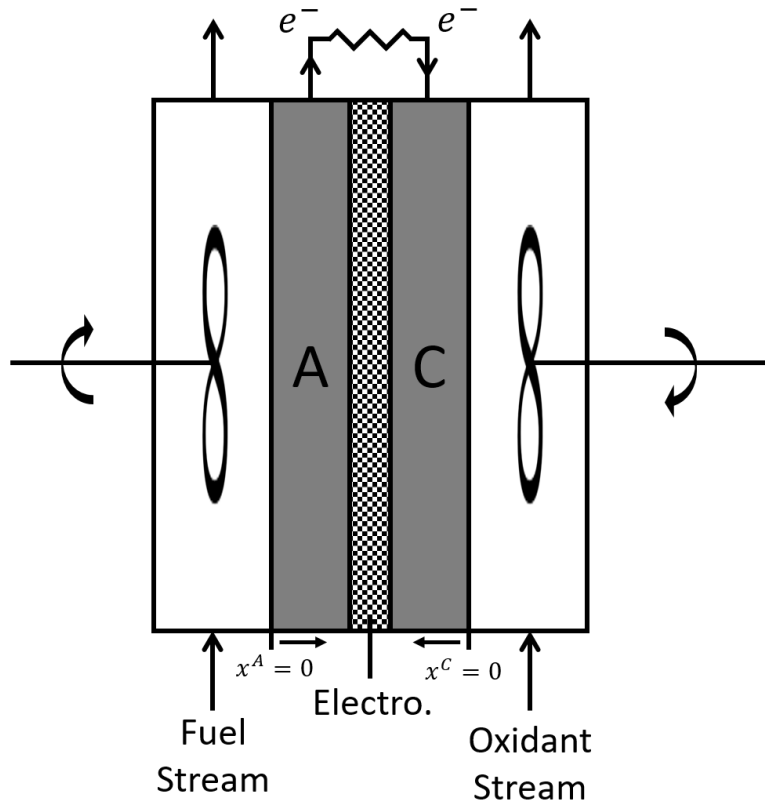


**Figure 1. Ideal solid oxide fuel cell as explained above.**

### 2. Formulation

The cell current,  $I$  (amperes), is assumed to be maintained at constant level corresponding to a required electric power,  $\dot{P}_{elec} = IV^{cell}$ , in the cell external load circuit. The required hydrogen consumption rate, in accordance with Eq. (2), is given by

$$\dot{n}_{H_2,cons} = \frac{I}{2F} \quad (3)$$

Therefore, at the steady-state SOFC cell operation, the required fuel gas feed rate = fuel consumption rate:

$$\dot{n}_{H_2,f} = \dot{n}_{H_2,cons} = \frac{I}{2F} \quad (4)$$

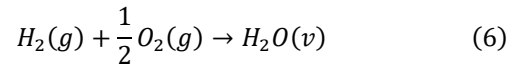
If the fuel feed from the fuel storage tank is impure; then,  $\dot{n}_{H_2,f}$  is given by

$$\dot{n}_{H_2,f} = (1 - y_{impurity})\dot{n}_{impure H_2} \quad (5)$$

Where  $\dot{n}_{impure H_2}$  is the feed rate of the impure fuel from the storage tank and  $y_{impurity}$  is the total mol fraction of all impurities present in the fuel stream.

For every one g-mole of fuel (hydrogen gas) consumed, one g-mole of water vapor is produced according to the reaction, Eq. (2). The reaction produced water vapor returns to the cell anode-side fuel compartment. At the cell steady-state, isothermal operational conditions; the gas mixture total pressure,  $p_{tot}^A$ , and total fuel (hydrogen gas) amount remain invariant.

Addition of Eq. (1) and (2) leads to:



This is the overall SOFC cell reaction. To deliver the cell current at the level of  $I$  (amperes), the conversion rate of oxygen must be

$$\dot{n}_{O_2,cons} = \frac{1}{2}\dot{n}_{H_2,cons} = \frac{I}{4F} \quad (7)$$

If the oxidant (oxygen) feed rate to the cell cathode-side compartment is at the excess oxygen fractional level of  $y_{O_2,ex}$  (e.g. 0.05 = 5 mol%), the required oxygen feed rate to the cell cathode-side compartment is given by:

$$\dot{n}_{O_2,f} = \left[ (1 + y_{O_2,ex}) \frac{I}{4F} \right] \quad (8)$$

The required dry air feed rate to the cell cathode-side compartment is:

$$\dot{n}_{dry\ air,f} = \frac{\dot{n}_{O_2,f}}{y_{O_2(in\ dry\ air)}} = \left[ \left( \frac{1 + y_{O_2,ex}}{y_{O_2(in\ dry\ air)}} \right) \frac{I}{4F} \right] \quad (9)$$

For oxidation or combustion calculations, it is acceptable to use  $y_{O_2(in\ dry\ air)} = 0.21$ . The atmospheric air has the following composition (in the chemical species mole fractions) [5]:

$$y_{N_2} = 0.7803 ; y_{O_2} = 0.2099 ; y_{Ar} = 0.0094 ; y_{CO_2} = 0.0003 ; \sum_{j=1}^5 y_j = 0.0001$$

Where  $j = H_2, He, Ne, Kr, Xe$ ; ( $j = 1$  to  $5$ ).

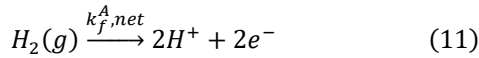
Dry air average molecular weight,  $M_{dry\ air} = 29.0\ g/mol$ .

If the air feed contains water vapor, the required feed rate of the moist air is:

$$\dot{n}_{moist\ air} = \frac{\dot{n}_{dry\ air}}{1 - y_{H_2O(in\ moist\ air)}} = \left[ \frac{1 + y_{O_2,ex}}{y_{O_2(in\ dry\ air)}(1 - y_{H_2O(in\ moist\ air)})} \right] \frac{I}{4F} \quad (10)$$

### The SOFC Electrode Electrochemical Reaction Kinetics:

During the SOFC operational period to deliver the required electric power to an external electrical load, the overall electrochemical reaction occurring in the porous anode of the cell is represented by:



It is here assumed that the reaction, Eq. (6), is first-order with respect to the molar concentration of hydrogen gas in the pores of the SOFC anode electrocatalyst. The developed mathematical expression for the hydrogen conversion rate; via the reaction; per unit volume of the cell porous anode is given by:

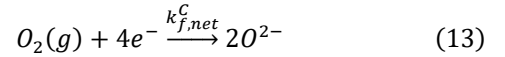
$$(-R_{H_2,net}) = k_{f,net}^A \frac{p_{tot}^A y_{H_2}}{RT} S_{eff}^A \rho_b^A \quad (12)$$

Where  $k_{f,net}^A$  is the net overall reaction rate coefficient ( $m_{pore}^3 \cdot m_{interface}^{-2} \cdot s^{-1}$ ),  $S_{eff}^A$  is the effective electroactive interfacial area per unit solid mass of the cell anode ( $m_{interface}^2 \cdot kg^{-1}$ ),  $\rho_b^A$  is the bulk solid mass density of the cell anode ( $kg \cdot m_b^{-3}$ ),  $p_{tot}^A$  is the total gas pressure in the cell porous anode ( $N \cdot m^{-2}$ ),  $R$  is the gas constant ( $8.314\ J \cdot mol^{-1} \cdot K^{-1}$ ),  $T$  is the cell operational temperature ( $K$ ), and  $y_{H_2}$  is the mol fraction of

hydrogen in the mixture of hydrogen and water vapor generated in in the reaction Eq (2).

From the reaction, Eq. (2), it is quite obvious that the consumption of every one mole of hydrogen produces one mole of water vapor; which, in turn, is transported to the anode-side fuel compartment via the molecular-mass diffusion process through the gas phase mixture present in the pores of the cell anode-electrode. Consequently, there is ‘no change’ in the gas mixture total pressure in the cell anode-side fuel compartment.

In the cell porous cathode, the oxidant (oxygen) is consumed via the following electrochemical reaction:



The conversion rate of oxygen via this reaction is given by

$$(-R_{O_2,net}) = k_{f,net}^C \frac{p_{tot}^C y_{O_2}}{RT} S_{eff}^C \rho_b^C \quad (14)$$

Where  $k_{f,net}^C$  is the net overall reaction rate coefficient ( $m_{pore}^3 \cdot m_{interface}^{-2} \cdot s^{-1}$ ),  $S_{eff}^C$  is the effective electroactive interfacial area per unit solid mass of the cell cathode ( $m_{interface}^2 \cdot kg^{-1}$ ),  $\rho_b^C$  is the bulk solid mass density of the cell cathode ( $kg \cdot m_b^{-3}$ ),  $p_{tot}^C$  is the total gas pressure in the cell porous cathode ( $N \cdot m^{-2}$ ), and  $y_{O_2}$  is the mol fraction of oxygen in the gas phase mixture present in the pores of the cathode.

### Predicting Hydrogen and Oxygen Mole Fraction Profiles within the Porous Anode and Cathode:

The hydrogen mole balance was applied over a spatial element of thickness,  $\Delta x^A$ , in the cell porous anode under the steady-state, isothermal conditions to obtain the following differential equation in the dimensionless form:

$$\frac{d^2 \phi^A}{d\zeta^2} - \lambda^A \phi^A = 0 \quad (15)$$

With boundary conditions:

$$\begin{aligned} \phi^A &= 1 \text{ at } \zeta = 0 \\ \frac{d\phi^A}{d\zeta} &= 0 \text{ at } \zeta = 1 \end{aligned} \quad (16)$$

Here,  $\phi^A$  is the ratio of the fuel mol fraction to the fuel mol fraction at the anode surface (i.e. at  $x = 0$ ) (Eq. 17),  $\lambda^A$  is a dimensionless quantity that compares the reaction rate to the effective diffusion rate (Eq. 18), and  $\zeta$  is the dimensionless distance through the cell porous anode (Eq. 19).

$$\phi^A = \frac{y_{H_2}}{y_{H_2,0}} \quad (17)$$

## “Formulation of an Ideal Solid Oxide Fuel Cell”

$$\lambda^A = \frac{k_{f,net}^A S_{eff}^A \rho_b^A (\ell^A)^2}{D_{eff,H_2}^A} \quad (18)$$

$$\zeta = \frac{x}{\ell^A} \quad (19)$$

Where  $\ell^A$  is the thickness of the anode and  $D_{eff,H_2}^A$  is the effective diffusivity of the fuel as determined from the true diffusivity  $D_{H_2}$ , the tortuosity,  $\tau^A$ , and the pore volume fraction of the cell porous anode,  $\varepsilon^A$  (Eq. 20).

$$D_{eff,H_2}^A = \frac{D_{H_2} \varepsilon^A}{\tau^A} \quad (20)$$

Solving the differential equation in Eq. 15 with boundary conditions in Eq. 16 yields the following solution of the dimensionless fuel mol fraction vs. fractional depth in the anode (Eq. 21).

$$\phi^A = \frac{e^{\zeta\sqrt{\lambda^A}} + e^{(2-\zeta)\sqrt{\lambda^A}}}{1 + 2\sqrt{\lambda^A}} \quad (21)$$

In the cell porous cathode, the molecular oxygen diffuses towards the cell electrolyte separator while being consumed via the net, assumed first-order reaction with respect to its molar concentration, Eq. (16). The oxygen mole balance was applied over a spatial element of thickness,  $\Delta x^C$ , in the cell cathode for the cell steady-state, isothermal operational conditions to obtain the following differential equation in the dimensionless form.

$$\frac{d^2\psi^C}{d\xi^2} - \lambda^C \psi^C = 0 \quad (22)$$

With boundary conditions:

$$\psi^C = 1 \text{ at } \xi = 0$$

$$\frac{d\psi^C}{d\xi} = 0 \text{ at } \xi = 1 \quad (23)$$

Here,  $\psi^C$  is the ratio of the oxidant mol fraction to the oxidant mol fraction at the cathode surface (i.e. at  $x = 0$ ) (Eq. 24),  $\lambda^C$  is a dimensionless quantity that compares the reaction rate to the effective diffusion rate (Eq. 25), and  $\xi$  is the dimensionless distance through the cell porous cathode (Eq. 26).

$$\psi^C = \frac{y_{O_2}}{y_{O_2,0}} \quad (24)$$

$$\lambda^C = \frac{k_{f,net}^C S_{eff}^C \rho_b^C (\ell^C)^2}{D_{eff,O_2}^C} \quad (25)$$

$$\xi = \frac{x}{\ell^C} \quad (26)$$

Where  $\ell^C$  is the thickness of the cathode and  $D_{eff,O_2}^C$  is the effective diffusivity of the oxidant as determined from the true diffusivity  $D_{O_2}$ , the tortuosity,  $\tau^C$ , and the pore volume fraction of the cell porous cathode,  $\varepsilon^C$  (Eq. 27).

$$D_{eff,O_2}^C = \frac{D_{O_2} \varepsilon^C}{\tau^C} \quad (27)$$

As the differential equation (Eq. 22) and boundary conditions (Eq. 23) are the same as those for the anode, the solution of the dimensionless oxidant mol fraction vs. fractional depth in the cathode is identical to the anode solution (Eq. 28).

$$\psi^C = \frac{e^{\xi\sqrt{\lambda^C}} + e^{(2-\xi)\sqrt{\lambda^C}}}{1 + 2\sqrt{\lambda^C}} \quad (28)$$

### 3. NUMERICAL DATA GENERATION FROM THE DEVELOPED FORMULATION

From Eq. (18), it is obvious that the dimensionless parameter for both the anode and cathode, the dimensionless parameter,  $\lambda$ , is proportional to  $k_{f,net}/D_{eff}$ . Since the reaction rate constant can be represented using an Arrhenius relationship [6, 7]:

$$k_{f,net} = A_{f,net} e^{\frac{E_{f,net}}{RT}} \quad (29)$$

And diffusion is proportional to  $T^{3/2}$  [8], the dimensionless parameter can then be represented as:

$$\lambda \propto \frac{e^{\frac{E_{f,net}}{RT}}}{T^{\frac{3}{2}}} \quad (30)$$

Therefore, different values of the parameter  $\lambda$  for both the anode and the cathode can be understood to represent different cell temperatures and how these operating conditions effect the relative rate of the electrochemical reaction and the diffusivity of the fuel/ oxidant species. **Figure 2** displays the behavior of  $\phi^A$  (or  $\psi^C$ ) as a function of  $\zeta$  (or  $\xi$ ) at different values of  $\lambda^A$  (or  $\lambda^C$ ).

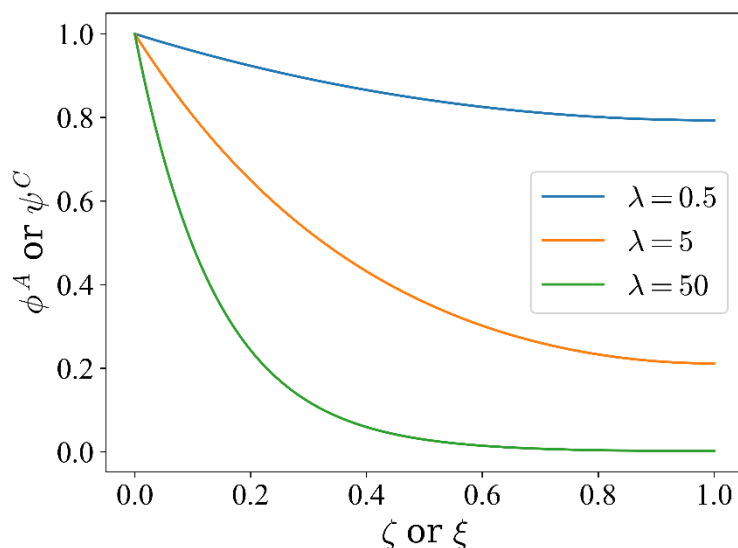


**Figure 2. Plots of the fuel/ oxidant mol fraction ratio vs. depth in the anode/ cathode at different values of  $\lambda$  (representing different cell temperatures)**

It is apparent that the mol fraction of the fuel/ oxidant species decreases as one moves from the solid anode/ cathode surface towards the electrode. Also apparent is that increasing the dimensionless parameter  $\lambda$  (equivalent to increasing the cell temperature) yields lower concentration profiles. This means an increase in the fuel/ oxidant conversion rate locally in accordance with the coupled effect of the reaction kinetics and its mass diffusion within the porous cell.

#### 4. CONCLUDING REMARKS

The formulation presented in this relatively short paper is for an ideal SOFC sketched in **Figure 1**. Using the presented formulation, one can calculate both the fuel (e.g. hydrogen gas) and oxidant (e.g. air) molar flow rates necessary to deliver a required cell current level. The formulation is also capable of predicting the fuel and oxidant mole fraction profiles in the cell porous anode and cathode electrode by accounting for the coupled effect of the intrinsic chemical/electrochemical kinetics and the effective diffusion of the reactant species in terms of the dimensionless parameter  $\lambda$ .

It is here suggested that a SOFC, of the type sketched in **Figure 1**, be constructed for testing the various fuel types (e.g. hydrogen, carbon monoxide, hydrocarbons, etc. as well as their mixtures) with the overall objective of determining their electric-energy delivery efficiency. The fully instrumented fuel cell of the type mentioned above can be used for the determination of the intrinsic chemical/electrochemical kinetics of the fuel oxidation process; the very significant information

always required for the development of the theory-based models to predict the performance behavior of a SOFC.

#### REFERENCES

1. S.S. Sandhu, K.R. Hinkle. Model for Prediction of Performance Behavior of a Solid Oxide Electrolyte Fuel Cell. *Submitted* (2023).
2. S.S. Sandhu, K.R. Hinkle. High Temperature Solid Oxide Electrolyte Fuel Cell Formulation: Non-steady state Utilization of Fuel and Oxidant. *In preparation* (2023).
3. A.J. Appleby, F.R. Foulkes. Fuel Cell Handbook, p. 588 (1989); Van Nostrand Reinhold.
4. P. Han et al. Novel oxide fuel cells operating at 600-800°C. An EPRI-GRI Fuel Cell Workshop on Fuel Cell Technology Research and Development, New Orleans (1993).
5. R.H. Perry, D.W. Green, Eds. Perry's Chemical Engineers' Handbook, pp. 9-3 through 9-54; 6<sup>th</sup> edition (1984), McGraw-Hill, New York.
6. H.S. Fogler. Elements of Chemical Reaction Engineering, pp.813-827; (2006, 4<sup>th</sup> edition), Prentice Hall.
7. J. Newman, N.P. Balsara. Electrochemical Systems, pp. 167-170; (2021, 4<sup>th</sup> edition), John Wiley & Sons, Inc.
8. R.B. Bird, W.E. Stewart, E.N. Lightfoot. Transport Phenomena, pp.582-590; (2007, 2<sup>nd</sup> revised edition), John Wiley & Sons, Inc.